Computers in Biology and Medicine 43 (2013) 1793–1803

Contents lists available at ScienceDirect

Computers in Biology and Medicine

journal homepage: www.elsevier.com/locate/cbm

IVUSAngio Tool: A publicly available software for fast and accurate 3D reconstruction of coronary arteries

Charalampos Doulaverakis [a,*], Ioannis Tsampoulatidis [a,1], Antonios P. Antoniadis [b,2], Yiannis S. Chatzizisis [b,**], Andreas Giannopoulos [b], Ioannis Kompatsiaris [a,1], George D. Giannoglou [b,2]

[a] Information Technologies Institute, Center for Research and Technology Hellas, 6th km Charilaou-Thermi road, 57001, Thermi, Thessaloniki, Greece
[b] Cardiovascular Engineering and Atherosclerosis Laboratory, First Department of Cardiology, AHEPA University Hospital, Aristotle University Medical School, 1 Stilponos. Kyriakidi Street, 54636, Thessaloniki, Greece

ARTICLE INFO

Article history:
Received 17 January 2013
Accepted 18 August 2013

Keywords:
Coronary angiography
Intravascular ultrasound
3D reconstruction
Software

ABSTRACT

There is an ongoing research and clinical interest in the development of reliable and easily accessible software for the 3D reconstruction of coronary arteries. In this work, we present the architecture and validation of *IVUSAngio Tool*, an application which performs fast and accurate 3D reconstruction of the coronary arteries by using intravascular ultrasound (IVUS) and biplane angiography data. The 3D reconstruction is based on the fusion of the detected arterial boundaries in IVUS images with the 3D IVUS catheter path derived from the biplane angiography. The *IVUSAngio Tool* suite integrates all the intermediate processing and computational steps and provides a user-friendly interface. It also offers additional functionality, such as automatic selection of the end-diastolic IVUS images, semi-automatic and automatic IVUS segmentation, vascular morphometric measurements, graphical visualization of the 3D model and export in a format compatible with other computer-aided design applications. Our software was applied and validated in 31 human coronary arteries yielding quite promising results. Collectively, the use of *IVUSAngio Tool* significantly reduces the total processing time for 3D coronary reconstruction. *IVUSAngio Tool* is distributed as free software, publicly available to download and use.
© 2013 Elsevier Ltd. All rights reserved.

1. Introduction

Coronary angiography and intravascular ultrasound (IVUS) are complementary modalities for coronary imaging, both suffering inherent diagnostic limitations. Coronary angiography only illustrates the silhouette of the contrast-filled lumen and fails to visualize the wall and quantify plaque burden [1]. IVUS offers accurate cross-sectional views of the arterial lumen and plaque, but its two-dimensional nature does not address the true three-dimensional (3D) coronary morphology [2,3]. An accurate and clinically relevant 3D representation of coronary arteries [4,5] which overcomes the inherent limitations of angiography and IVUS would be very useful in atherosclerosis. Early attempts in this area employed simple stacking of IVUS images to create a linear 3D arterial outline [6,7] providing no information about the spatial configuration of the reconstructed vessel. A geometrically-correct 3D coronary reconstruction by fusing angiography and IVUS data also emerged. With this approach, biplane angiography images are combined to construct the 3D trajectory of the IVUS catheter, where the IVUS cross-sectional images are then aligned [8–14]. The geometrically-correct 3D reconstruction of coronary arteries has been experimentally and clinically validated [10,15–17].

Despite the considerable progress achieved, the application of 3D IVUS in clinical practice has been limited. This is largely attributed to software-related issues: some systems require initialization and calibration for the X-ray angiography system using phantom models [17], being impractical for everyday use; other applications run complicated interfaces requiring high technical expertise or significant training time [18]. Medical imaging vendors have been active in relevant software development [19,20] but until now no standalone application for 3D coronary reconstruction has been widely available.

Taking the above considerations into account, we developed a publicly available, user-friendly software called *IVUSAngio Tool*, which performs 3D reconstruction of coronary arteries using IVUS

* Corresponding author. Tel.: +30 2311257727; fax: +30 2310474128.
** Corresponding author. Tel./fax: +30 2310994837.
E-mail addresses: doulaver@iti.gr (C. Doulaverakis), itsam@iti.gr (I. Tsampoulatidis), aantoniadis@gmail.com (A.P. Antoniadis), joc@med.auth.gr (Y.S. Chatzizisis), andgiannop@hotmail.com (A. Giannopoulos), ikom@iti.gr (I. Kompatsiaris), yan@med.auth.gr (G.D. Giannoglou).
[1] Tel.: +30 2311257700; fax: +30 2310474128
[2] Tel./fax: +30 2310994837.

0010-4825/$ - see front matter © 2013 Elsevier Ltd. All rights reserved.
http://dx.doi.org/10.1016/j.compbiomed.2013.08.013

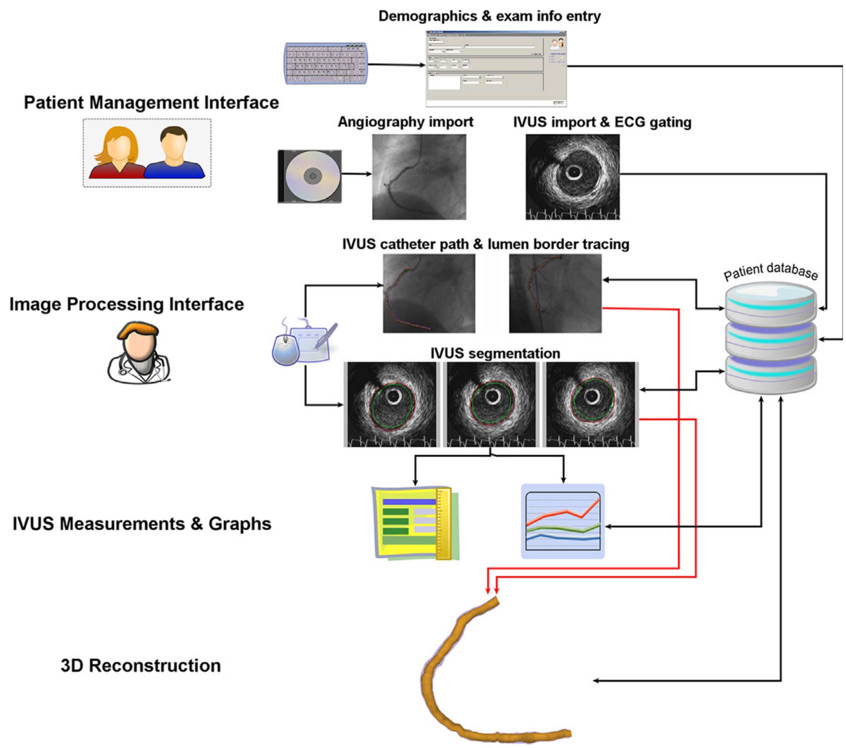

Fig. 1. The process for the 3D reconstruction of a coronary vessel.

and biplane angiography. *IVUSAngio Tool* also offers useful 3D artery visualization options, such as localization of the 2D IVUS images on the 3D model (2D–3D correspondence) and fly-through imaging. The programming methodology is generic, thus the software can use data from different angiography and IVUS vendors. Also, the software functions are developed in a modular way allowing easy export of the IVUS analyses and the reconstructed 3D arteries in third-party applications. The software functionality and features have been evaluated using a large patient dataset. *IVUSAngio Tool* is freely available at the website http://mklab.iti.gr/ivus.

The paper is organized as follows: Section 2 gives an overview of IVUSAngio Tool's design and usage and details its implementation. Section 3 describes the patient management and data import procedure. In Section 4 a description of the biplane angiography processing functionality is given, while in Section 5 the IVUS processing procedure is described and detailed description of the implemented algorithms is given. Section 6 outlines the 3D reconstruction capability, the 3D model manipulation options and the implemented algorithms, while Section 7 describes the embedded 3D viewer. Section 8 presents the validation that was performed on the Tool. Section 9 discusses the results and the paper is concluded with Section 10.

2. Software architecture

Fig. 1 presents an outline of the software functions. Patient management and data import modules handle the patient information and angiography/IVUS data import. The software performs a fully automatic selection of end-diastolic IVUS frames. The IVUS catheter path and lumen borders are semi-automatically tracked in two orthogonal angiography projections (i.e. left and right anterior oblique) acquired prior to the beginning of the IVUS pullback. The lumen and media-adventitia borders are traced in the IVUS images with either a semi-automated or a fully automated approach. The angiography and IVUS data are appropriately combined resulting in the 3D reconstructed coronary artery. Finally, the software calculates and exports several arterial morphometric parameters and presents them graphically.

The patient management module, the angiography and IVUS processing modules and the 3D reconstruction component are all integrated in a user-oriented graphical interface. *IVUSAngio Tool* was developed in C++. Additional APIs used are Intel's OpenCV [21] for image manipulation and computer vision algorithms, the Imebra library [22] for DICOM file handling and the SISL library [23] for B-splines manipulation. The 3D reconstruction system was developed in the OpenGL library [24]. *IVUSAngio Tool* runs on the Windows® operating system. Notably, *IVUSAngio Tool* can run on portable storage devices, such as removable hard drives, USB memory sticks, or SD cards and the patient database can be exported and accessed across different workstations.

3. Patient management and data import

3.1. Patient information, angiography and IVUS import

The patient management module uses an input interface (Fig. 2a) for patient data, such as the patient identification number, name, date of birth, laboratory results, and angiography/IVUS information. Via an integrated DICOM viewer, the user displays and imports the angiography and IVUS data (Fig. 2b). Angiography and IVUS data can also be imported from avi video or jpeg image files.

3.2. Automatic selection of end-diastolic IVUS images

Manual selection of end-diastolic IVUS frames is a time-consuming and laborious process and therefore a rate-limiting step in the automated 3D reconstruction of coronary arteries. To facilitate and accelerate this process, we developed an automatic end-diastolic IVUS frame selection algorithm using ECG, embedded on the IVUS images. Prefiltering, interframe difference and adaptive thresholding

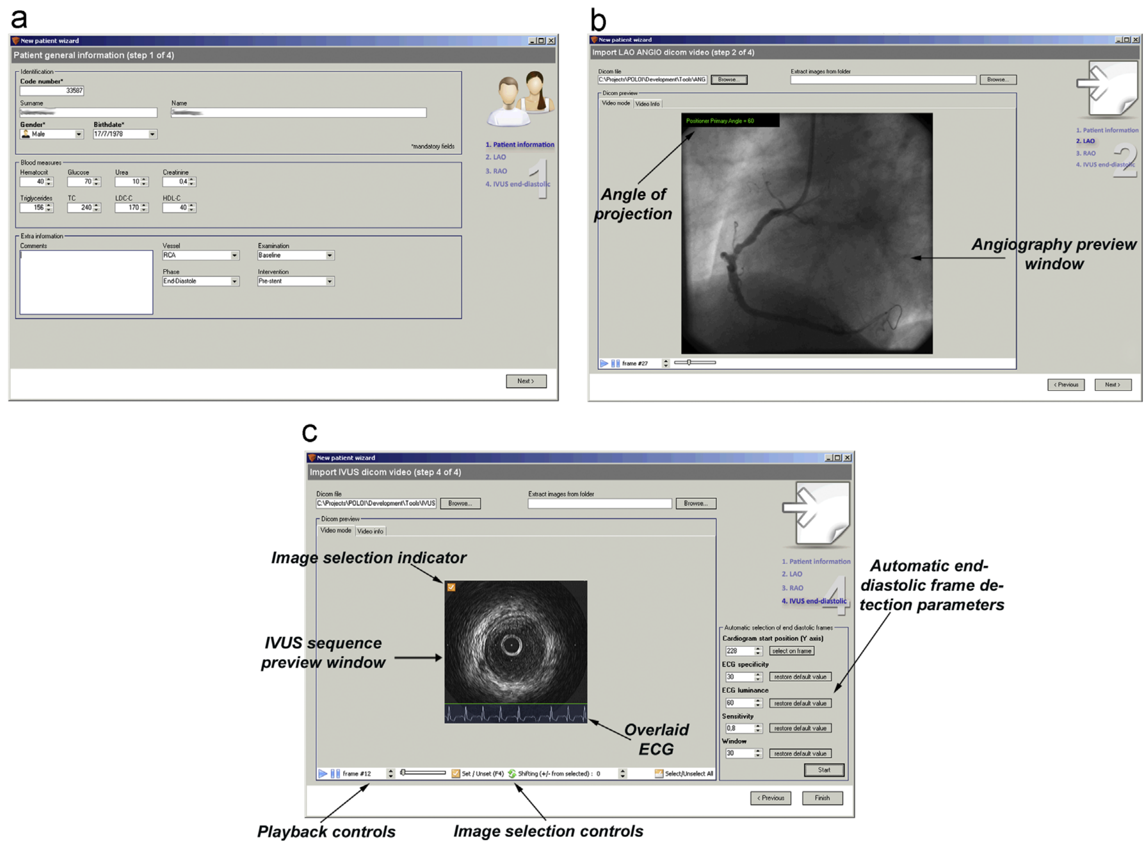

Fig. 2. New patient generation wizard. (a) Medical record data, (b) angiography video, (c) IVUS sequence and end-diastolic frame selection.

are implemented in a sliding window approach to identify the end-diastolic frames on the basis of the R-wave detection (Fig. 2c). Manual corrections of the selected frames can be done. Shifting the entire detected set at a given number of frames is also available, thus enabling immediate focusing on any phase of the cardiac cycle. The software also allows manual frame selection in case the ECG is not provided along with the IVUS.

4. Angiography image processing

Fig. 3a displays the user interface for angiography image processing which provides the following features:

4.1. Calibration setting

To calibrate the angiographic images, the user marks the dimensions of any fixed distance within the angiographic image. The width of the angiography diagnostic catheter is commonly used for this purpose.

4.2. Image enhancement controls and zooming

Angiographic images may not be optimal for analysis due to poor image contrast or brightness likely making the catheter tracking troublesome. For this purpose, several image enhancement controls have been implemented to adjust image contrast, brightness and gamma settings. Zoom in and zoom out features are also available.

4.3. Point-and-click catheter and lumen borders tracking

A point-and-click interface allows manual detection of the IVUS catheter and lumen borders, which are then interpolated with B-spline curves [25]. Undo, redo, point deletion and point movement options are also available.

5. IVUS image processing

Fig. 3b shows the graphical environment for IVUS image processing which provides the following features:

5.1. Calibration

To calibrate IVUS images the user defines the center and width of the IVUS catheter and also calculates the scaling factor using a fixed distance within the image, such as the IVUS catheter diameter or the length between calibration markers.

5.2. IVUS image segmentation

Manual IVUS segmentation is a time-consuming process and therefore a major rate-limiting step in the 3D reconstruction of coronary arteries. We developed a semi-automatic and fully automatic IVUS segmentation algorithm incorporated in the software interface.

5.2.1. Semi-automatic IVUS segmentation

In this functionality, the user delineates an initial hand-drawn estimate of the contour, which is then fitted to the actual boundaries by employing deformable contours techniques [26]. The starting and ending points of the outlined border are

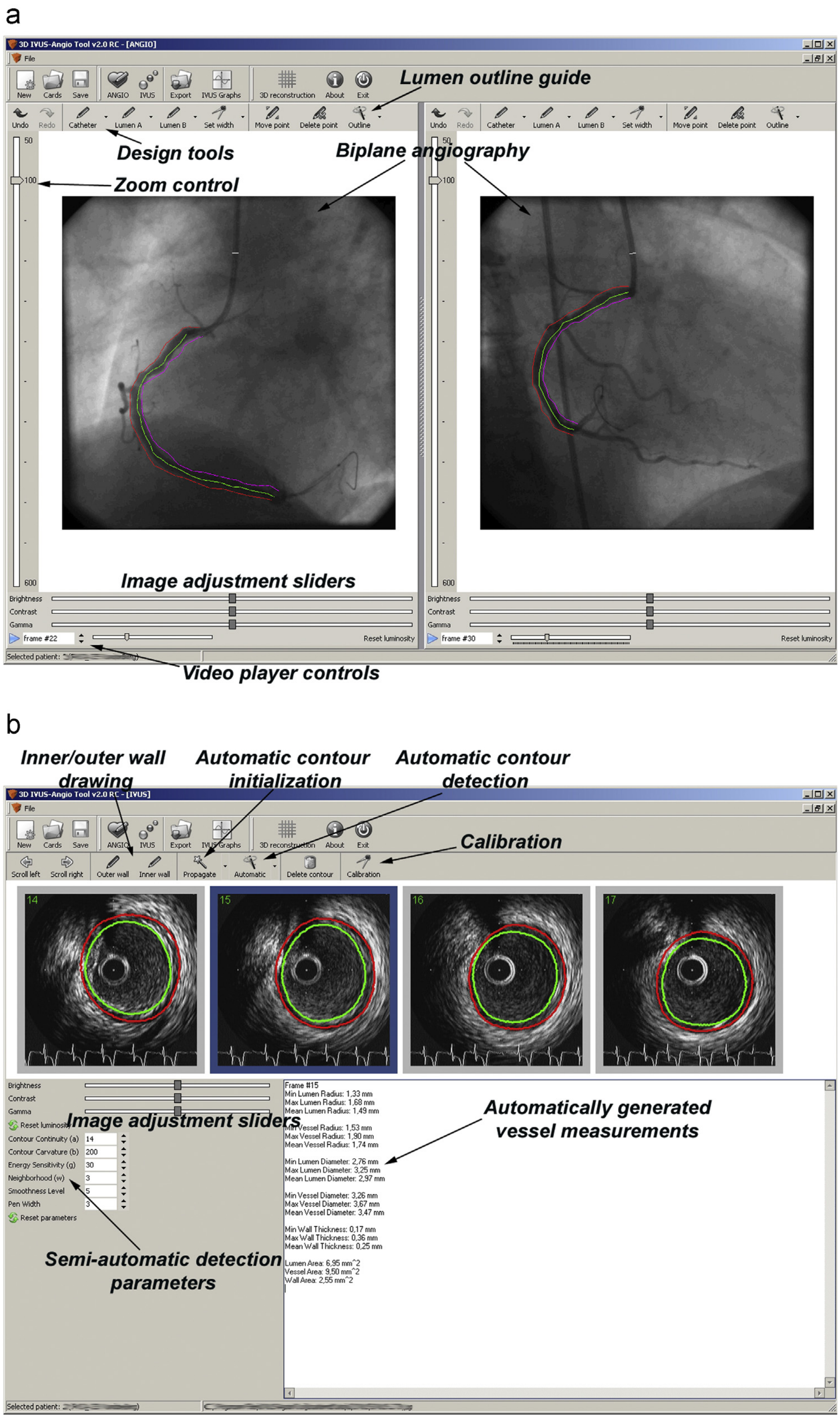

Fig. 3. IVUSAngio Tool interface. (a) Angiography processing, (b) IVUS processing. Interface design and functionalities. In semi-automatic IVUS segmentation an initial hand-drawn contour, fits to the actual boundaries by employing deformable contours techniques. Graphical controls adjust parameters like Contour Continuity (how much each contour point is allowed to move further from its neighbors), Contour Curvature (the weight that allows the contour to have corners), Energy sensitivity (the sensitivity of the contour to image intensity changes), Neighborhood (the window where the image gradient is calculated), and Smoothness Level (the amount of smoothing applied to the curve).

connected with B-spline approximation and the contour is further refined by applying low-pass filtering to produce a smooth curve. This approach has been implemented and validated in vivo [27,28].

The extent of the deformation force and smoothing level that is applied to the contours are adjusted through appropriate graphical controls (Fig. 3b). An auto-initialization contour option is also

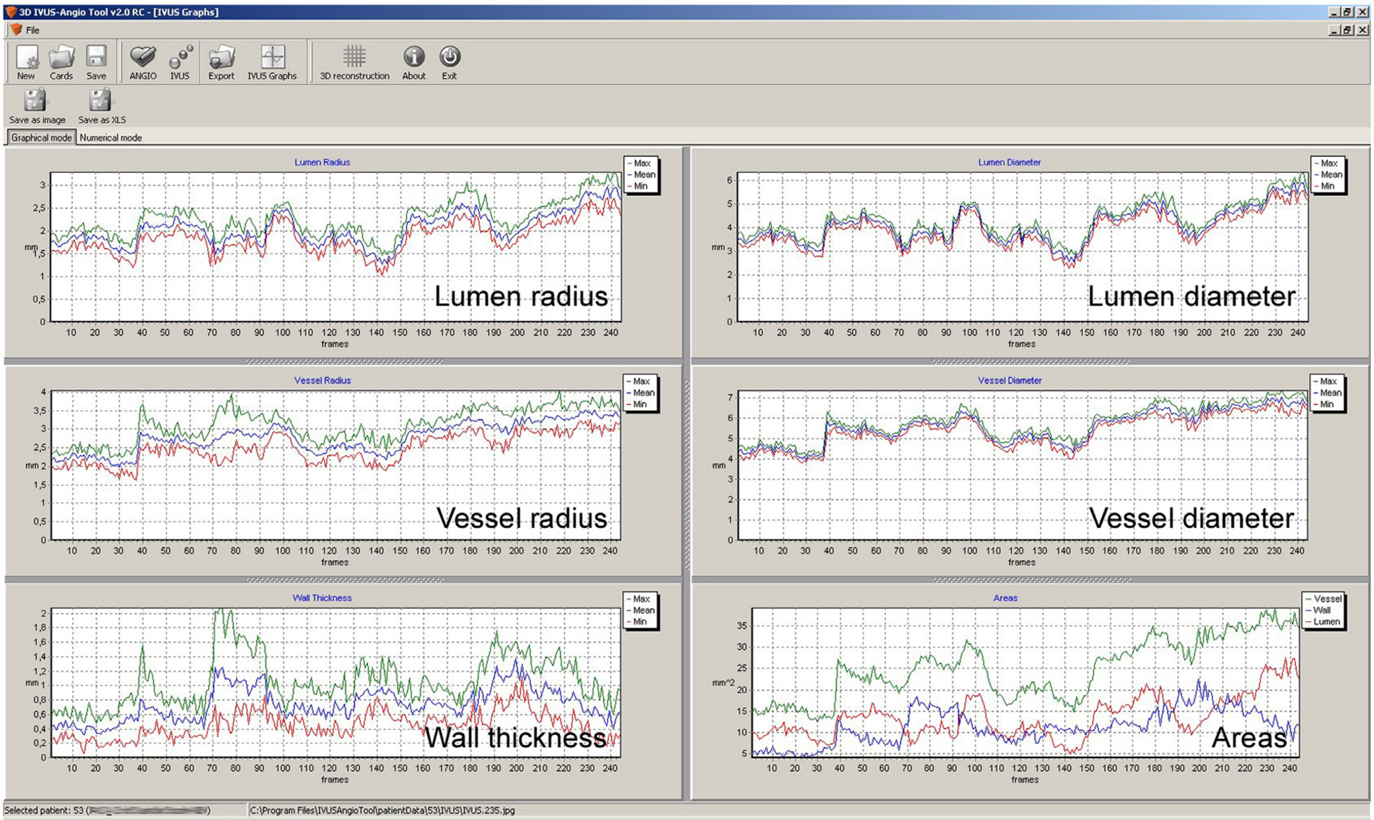

Fig. 4. Automatically generated morphometric measurements of IVUS images.

available to accelerate detection, where a satisfactory segmentation contour is used as initial contour for the next frames (propagation) and is deformed to match the new frame, thus alleviating the need for manual delineation.

5.2.2. *Automatic IVUS segmentation*

The texture-based automatic IVUS contours detection method requires no user intervention and has been previously been reported and validated [29]. Briefly, the IVUS images are transformed in polar coordinates and truncated in order to remove the catheter. A four level Discrete Wavelet Frames analysis is performed with a filter bank based on the low-pass Haar filter $H(z)=\frac{1}{2}(1+z^{-1})$ to extract specific texture features. The inner and outer contours are initialized using texture and luminance features. The initialized contours are further refined by applying successive low-pass filtering. Graphical controls adjust the smoothing level of the final contours, the intensity threshold for the detection of the outer contour and the number of consecutive images that the method will be applied to.

5.3. *Graphical visualization of IVUS measurements*

IVUS morphometric measurements are automatically displayed on screen (Fig. 3b). These include minimum, maximum and mean lumen radius, vessel radius and wall thickness, together with lumen, vessel and wall areas. Following the segmentation of IVUS images for the entire artery, a spreadsheet with the above measurements is created on demand. Also, graphical plots of these parameters are automatically generated (Fig. 4), facilitating the visual identification of vascular morphological abnormalities in the longitudinal axis.

6. User interface for 3D reconstruction

The 3D model reconstruction is automatically performed with a single click on the *IVUSAngio Tool* interface, by fusion of the angiography and IVUS analysis data (Fig. 5). Intermediate steps for 3D model generation are:

6.1. *3D reconstruction of the IVUS catheter path*

The 3D reconstruction of the IVUS catheter trajectory is accomplished with the use of epipolar geometry rules as previously described [30].

6.2. *Placement and relative orientation of IVUS contours*

The IVUS contours are placed along the 3D reconstructed IVUS catheter path. Each pair of contours is placed on a plane perpendicular to the catheter path at the given point. The distance of each contour from the pullback start point is calculated with the following formula:

$$\text{Distance (mm)} = \frac{\textit{IVUS Frame Number}}{\textit{Total Number of IVUS Frames}} \times \textit{IVUS Pullback Length}\ \text{(mm)} \quad (1)$$

Subsequently, the relative orientation of each contour with respect to the 3D catheter path is estimated using the Frenet–Serret formulas [9].

6.3. *Absolute rotation*

Following relative orientation, the absolute rotation of the entire contours set is calculated. This is accomplished by successive rotations and back-projections of the reconstructed lumen to the angiography planes where each projection is compared to the

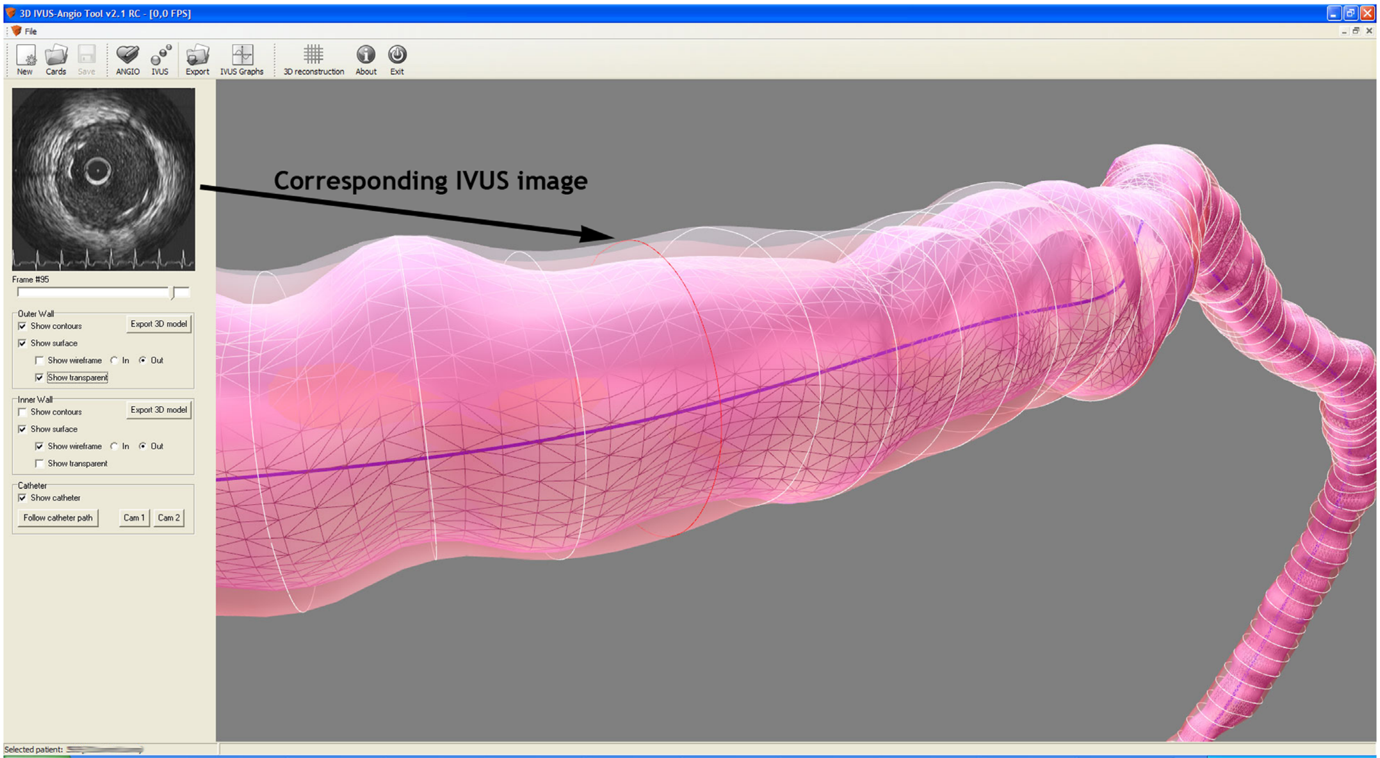

Fig. 5. 3D reconstructed coronary artery. The correspondence between 2D IVUS images and the selected IVUS contour (arrow) on the 3D reconstructed artery is depicted.

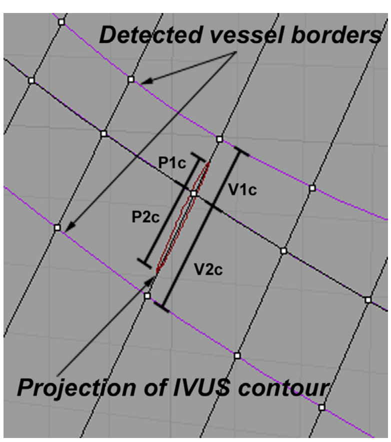

Fig. 6. Projection error calculation.

actual luminal silhouette in angiography (Fig. 6). The angle which presents the smallest cumulative error e_ϑ for both projections according to Eq. (2) is the absolute rotation angle ϑ of the contours

$$e_\vartheta = \sum_{c\vartheta}(|P1_{c\vartheta} - V1_{c\vartheta}| + |P2_{c\vartheta} - V2_{c\vartheta}|) \quad (2)$$

in which *V1* and *V2* are the distances between the catheter and the detected luminal contours and *P1* and *P2* the distances between the catheter and the back-projected luminal edges.

6.4. Surfaces generation and rendering

NURBS surfaces are generated in real time through the inner and outer IVUS contours forming the lumen and media-adventitia surfaces respectively.

7. 3D viewer

Regarding the integrated 3D viewer in *IVUSAngio Tool*, several functionalities have been implemented in order to enhance user experience and visualization capabilities. These are:

7.1. 3D model browsing

Zooming and panning functionality is available using mouse dragging. Additionally the opacity of the media-adventitia, surface can be adjusted permitting the visual estimation of the vessel wall thickness.

7.2. 2D–3D correspondence

By clicking on any location in the 3D model, the user displays the corresponding IVUS image thus registering a side-by-side investigation of IVUS and 3D geometry (Fig. 5).

7.3. Fly-through camera

An inside view of the vessel is offered as a moving camera that follows the IVUS catheter path. Video rendering happens in real time and the IVUS frame that corresponds to the current camera position in the vessel is also displayed.

7.4. Additional functions

The model can be exported in *openNURBS* format for detailed numerical analysis in CAD applications. The angiography and IVUS coordinate data can be also exported in text/xml files.

Table 1
Sensitivity, specificity and diagnostic accuracy of the automatic ECG gating algorithm.

	Sensitivity	Specificity	Accuracy
Automatic ECG gating (n=21,319 images)	85.1% (95% CI: 83.8% to 86.3%)	96.4% (95% CI: 96.2% to 96.7%),	94.7%

Table 2
Comparison of automatic vs. manual segmentation of IVUS images. Values are mean ± SD. Regarding centroids coordinates, the reference point (0,0) was arbitrarily chosen as the upper left corner of each image.

	Lumen				Vessel			
	Manual segmentation	Automatic segmentation	Difference	p	Manual segmentation	Automatic segmentation	Difference	p
Area	6.17 ± 2.78 mm^2	6.19 ± 2.84 mm^2	1.24 ± 1.34 mm^2	<0.001	9.86 ± 4.40 mm^2	8.24 ± 3.33 mm^2	2.02 ± 1.98 mm^2	<0.001
Minimum diameter	2.52 ± 0.61 mm	2.69 ± 0.59 mm	0.32 ± 0.28 mm	<0.001	3.27 ± 0.79 mm	3.13 ± 0.66 mm	0.29 ± 0.31 mm	<0.001
Maximum diameter	2.82 ± 0.67 mm	2.83 ± 0.62 mm	0.29 ± 0.27 mm	<0.001	3.60 ± 0.85 mm	3.24 ± 0.67 mm	0.44 ± 0.35 mm	<0.001
Centroid x	3.45 ± 0.54 mm	3.49 ± 0.42 mm	0.19 ± 0.14 mm	-	3.47 ± 0.56 mm	3.48 ± 0.41 mm	0.22 ± 0.17 mm	-
Centroid y	3.11 ± 0.52 mm	3.14 ± 0.40 mm	0.20 ± 0.16 mm	-	3.11 ± 0.55 mm	3.14 ± 0.39 mm	0.23 ± 0.19 mm	-

8. Validation

8.1. Validation set-up

The *IVUSAngio tool* was validate in 5339 ECG-gated IVUS images derived from 31 human coronary arteries (RCA $n=11$, LAD $n=8$, LCX $n=12$). The study was compliant with the Helsinki Declaration and approved by the Institutional Ethics Committee. All subjects provided written informed consent for their participation in the study. The IVUS was performed with a mechanical imaging system (ClearView; Boston Scientific, Natick, Massachusetts, USA) and a 2.6 F sheath-based catheter, incorporating a 40 MHz single-element transducer and yielding 30 images/second (Atlantis SR Pro; Boston Scientific). A motorized pullback device was used to withdraw the catheter from its most distal location to the tip of the guiding catheter at a constant speed of 0.5 mm/s.

8.2. Validation of automatic ECG gating

Manual ECG gating was performed separately in all arteries by an expert cardiologist and the manually selected end-diastolic frames were compared with the automatically selected ones. The automatic detection algorithm yielded a sensitivity of 85.1% (95% Confidence Interval: 83.8% to 86.3%) and a specificity of 96.4% (95% Confidence Interval: 96.2% to 96.7%), and an accuracy of 94.7% for the selection of end-diastolic frames, clearly indicating that the automatic IVUS gating algorithm is highly accurate (Table 1).

8.3. Validation of automatic IVUS segmentation

The automated method of contour detection was validated in a large dataset of images ($n=5339$). Manual segmentation of this dataset of images by an independent IVUS expert was used as reference. The inter-observer agreement of manual segmentation was tested on a subset of 505 IVUS images from 11 patients. These images were manually segmented by two independent IVUS experts. The lumen and EEM measurements by the two independent experts demonstrated a highly significant degree of agreement (Lumen area: 5.57 ± 2.85 vs. 5.56 ± 2.90 mm^2, $p=0.83$, EEM area: 8.83 ± 4.27 vs. 8.85 ± 4.31 mm^2, $p=0.68$) with very high correlation (Lumen area: $y=0.97x+0.158$, correlation coefficient$=$ 0.95, $p<0.001$, EEM area: $y=0.97x+0.22$, correlation coefficient$=$ 0.98, $p<0.001$), clearly indicating the high accuracy of manual segmentation which was used as gold-standard for the validation of automatic segmentation.

Table 2 displays the mean absolute difference and standard deviation between ground truth manual segmentation and automatic detection results of lumen, vessel and wall areas, measured in mm^2 and the mean absolute difference and standard deviation between ground truth and automatic detection regarding the following descriptors of shape: minimum and maximum diameter and centroid location for lumen and vessel contours. The automatic segmentation results showed a good agreement with the ground truth values, especially for lumen borders where differences are relatively small. Figs. 7 and 8 show the Bland–Altman and linear regression plots of the semi-automatic versus automatic IVUS segmentation for area and shape parameters, respectively. The Bland–Altman plots were constructed with the manual segmentation method in the X-axis as suggested in the literature [31]. A high agreement between the two methods was found in the Bland–Altman plots for most geometric parameters. In addition to the Bland Altman plots, the linear regression analysis showed a significant association between the manual and automatic segmentation, with slopes close to 1.0 and intercepts varying between 0.5 and 1.5.

8.4. Overall time gain of 3D reconstruction of coronary arteries with IVUSAngio Tool

Table 3 displays the time gain in 3D reconstruction process with the use of *IVUSAngio Tool*. We compared the time required for manual 3D reconstruction with three *IVUSAngio Tool*-based 3D reconstruction approaches: a. fully automatic, b, automatic with manual corrections and c. semi-automatic. The automatic IVUS segmentation method in *IVUSAngio Tool* resulted in a time benefit of 70.5% versus manual segmentation. Also, we calculated the time required to carry out the segmentation in the scenario where each automatically segmented contours is user-corrected when it is $>15\%$ different in area than the manual segmentation. With this approach, there is a 35.2% time gain compared with the manual 3D reconstruction method, without compromising the accuracy of the results. The 3D reconstruction using semi-automatic IVUS segmentation yielded a time gain of 24.3% versus the manual 3D reconstruction.

9. Discussion

In this study we presented the *IVUSAngio Tool* software that performs fast and accurate 3D reconstruction of coronary arteries from IVUS and biplane angiography. Fully automatic IVUS gating and segmentation are important components of the software. Of note,

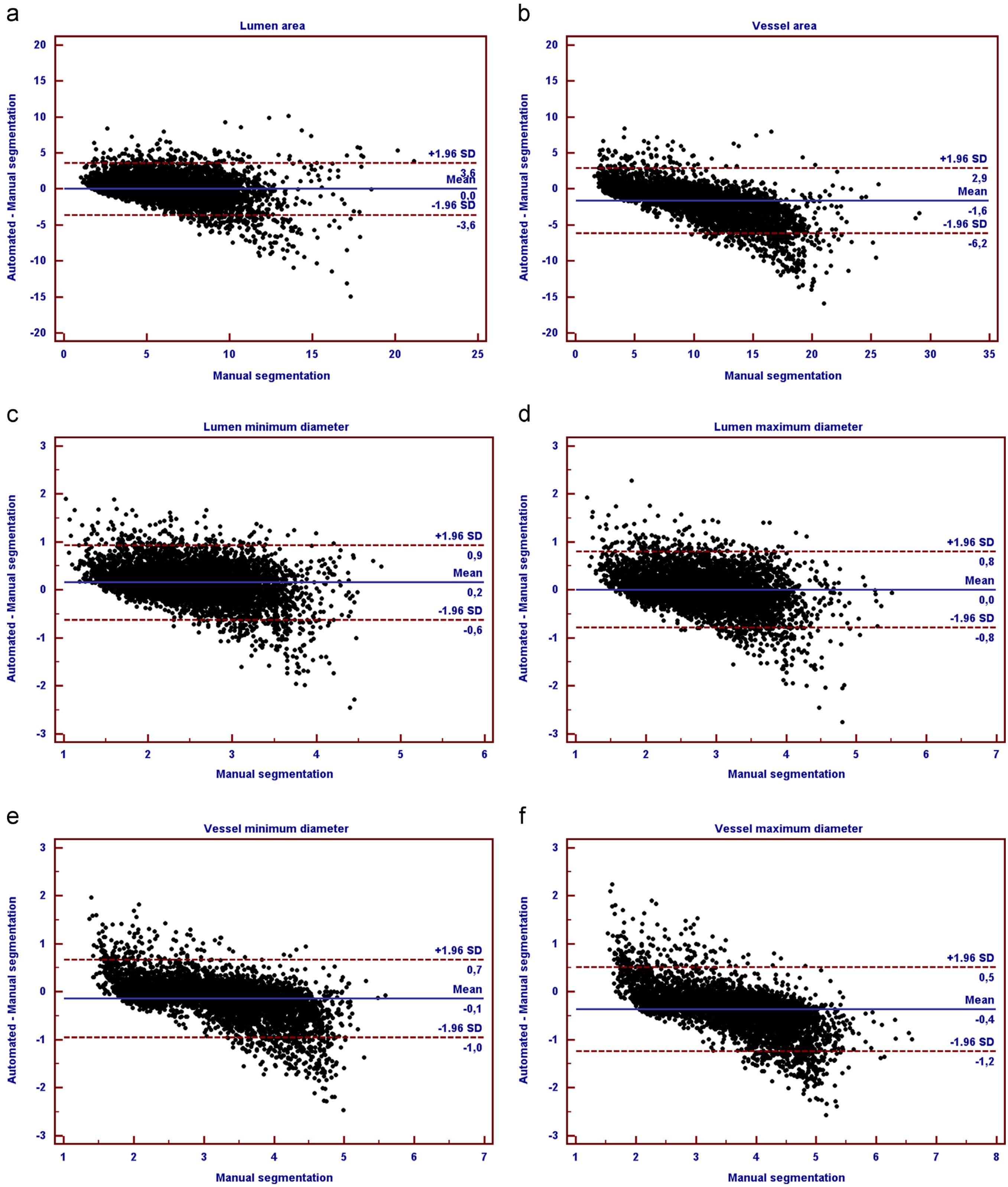

Fig. 7. plots of differences for the lumen and vessel areas, shape and min/max diameters. The mean differences (blue solid lines) between manual and automatic IVUS segmentation with the 95% limits of agreement (red dashed lines) are shown. The plots demonstrate that the mean difference between automated and manual segmentation is close to zero with the majority of the differences lying within these ±2SD (For interpretation of the references to color in this figure legend, the reader is referred to the web version of this article).

this software is publicly available for further development and use. The *IVUSAngio Tool* was tested in an extensive dataset of more than 5000 ECG-gated IVUS images derived from 31 human coronary arteries yielding significant accuracy in 3D reconstruction of coronary arteries. Both the automatic ECG gating algorithm and the automatic IVUS segmentation yielded very satisfactory outcomes compared to manual processing. Of equal importance, the software yielded a time benefit ranging from 24% to 70% in 3D reconstruction procedure.

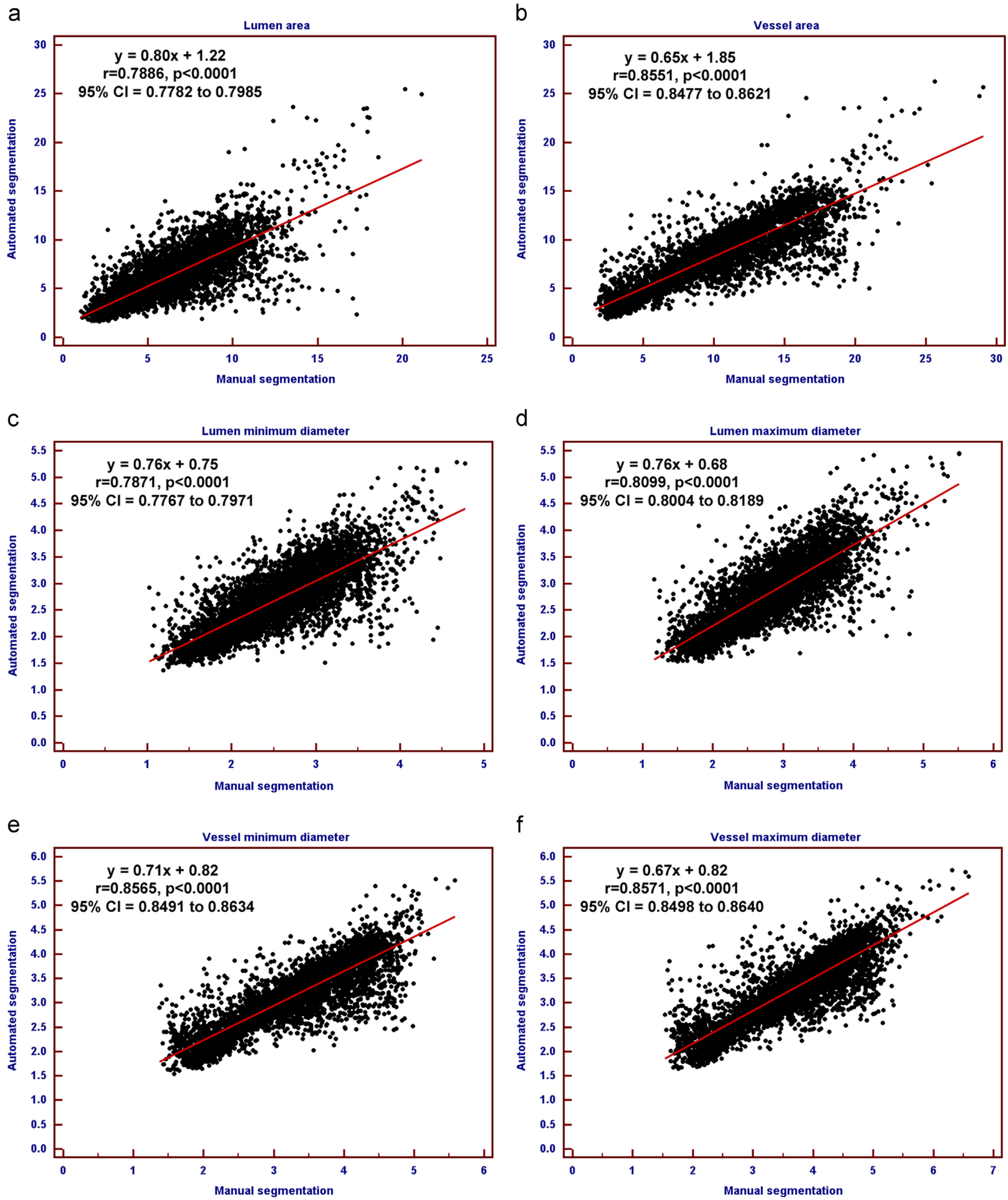

Fig. 8. Linear regression plots for the lumen and vessel areas and and min/max diameters. The graphs show a significant correlation between the manual and automatic segmentation of IVUS images with slopes close to 1.0 and intercepts varying between 0.5 and 1.5.Note that 95% CI refers to *r*.

There is a growing demand for readily available, accurate, reliable, rapid and non-complicated software for 3D coronary reconstruction. The majority of existing systems for 3D coronary reconstruction are proprietary and this may have accounted for the restriction of their potential target group and non-widespread use. *IVUSAngio Tool* may contribute to achieving the above clinical and

Table 3
Time gain of the automatic and semi-automatic 3D reconstruction methods provided by the *IVUSAngio Tool*. Comparisons of each method were done against manual reconstruction.

	Manual processing	Automatic IVUS processing	Time gain vs. manual	p	Automatic IVUS processing with manual correction	Time gain vs. manual	p	Semi-automatic IVUS processing	Time gain vs. manual	p
Data import (min/**case**)	6.5 ± 1.1	6.5 ± 1.1	0	–	6.5 ± 1.1	0	–	6.5 ± 1.1	0	–
ECG Gating (min/**case**)	25.2 ± 7.6	0.8 ± 0.2	96.2%	< 0.001	0.8 ± 0.2	96.2%	< 0.001	0.8 ± 0.2	96.2%	< 0.001
Angio Segmentation (min/**case**)	19.8 ± 5.1	19.8 ± 5.1	0	–	19.8 ± 5.1	0	–	19.8 ± 5.1	0	–
IVUS Segmentation (min/**case**)	102.6 ± 31.0	0.7 ± 0.2	99.3%	< 0.001	63.9 ± 19.3	37.7%	< 0.001	83.2 ± 25.1	18.9%	< 0.01
3D Reconstruction (min/**case**)	31.0 ± 9.4	31.0 ± 9.4	0	–	31.0 ± 9.4	0	–	31.0 ± 9.4	0	–
Total time (min/**case**)	**178.6 ± 52.8**	**52.4 ± 14.6**	**70.5%**	**< 0.001**	**115.5 ± 33.6**	**35.2%**	**< 0.001**	**134.9 ± 39.5**	**24.3%**	**< 0.001**

research targets as it implements a user-oriented approach, does not require particular user skills and expertise and it is freely distributed.

Three dimensional reconstruction of the coronary arteries carries important investigational and clinical implementation as it enables the study of factors which affect the progression of atherosclerosis and the natural history of atherosclerotic plaques [32–34]. In the clinical arena, the coronary 3D reconstruction method can yield rapid and more reliable morphometric plaque analysis improving the clinical individualized decision-making and stent-positioning quality [35]. Also, it can be applied to accurately follow-up the outcome of coronary interventions, e.g. stent placement, in the progression or regression of atherosclerosis and further explore the pathophysiology of in-stent restenosis [36].

In the research field, 3D reconstruction of coronary arteries is the foundation in the study of the role of local hemodynamics on atherosclerosis. As an initial application, a computational grid is generated on the 3D reconstructed arteries and the blood flow is simulated using computational fluid dynamics software with subsequent hemodynamic factors calculation, such as the endothelial shear stress and tensile stress, along the vascular wall [37,38]. Studies have shown that low endothelial shear stress is related to the development of high risk atherosclerotic plaques, i.e. with a high probability of rupture that would lead to acute coronary syndromes [39,40]. Specifically, an oscillatory and persistently low endothelial shear stress area with increased tensile stress precipitate the progression of atherosclerosis [39].

In the same artery, 3D reconstruction in both systole and diastole permits the calculation of coronary elasticity. Decreased elasticity (i.e. increased wall stiffness) is associated with negative remodeling and stenotic lesions while increased elasticity is linked to excessive expansive remodeling and development of high risk atherosclerotic plaques [39].

We acknowledge the limitation that the results shown in Table 3 are the outcomes by a single user of the software. However, the single-user segmentation outcomes were highly consistent with the results of a second user in a representative subset of the images. Also, the automatic segmentation algorithms, while promising, are amenable to further improvement.

10. Conclusions and future perspectives

IVUSAngio Tool is a user-friendly yet powerful, publicly available tool for coronary 3D reconstruction. Future work includes the development and integration of a computational fluid dynamics module for blood flow simulations in the reconstructed arterial geometry. Work towards integrating algorithms for automatic processing of Optical Coherence Tomography intravascular images is also being carried out [41]. Extensive testing and interaction with users in the medical community, providing feedback to the program development team has already contributed in making this software both easy to use and efficient. Free distribution is anticipated to sustain and enhance the *IVUSAngio Tool* use and evaluation and lead to further software development. A real-time 3D coronary reconstruction and flow dynamics analysis is the ultimate goal, as this will potentiate the use and applications of this method in the study and management of coronary artery disease.

Paper summary

IVUSAngio Tool is a software application for automated analysis of IVUS and coronary angiography to produce 3D reconstructions of coronary arteries. The Tool integrates functionalities such as automatic IVUS segmentation, calculation and extraction of morphometric arterial parameters, 3D model generation and exporting. All the above are presented in a user-friendly graphical environment. Extensive in-vivo validation of the software was performed showing that *IVUS Angio Tool* can accurately and rapidly reconstruct the coronary arteries providing important morphometric information of the coronary arteries that can be used for clinical and research purposes. Of note, the software is publicly available.

Conflicts of interest

None declared.

Acknowledgments

This project was funded by the General Secretariat of Research and Technology, Athens, Greece and by the Behrakis Foundation, Boston, USA.

References

[1] T. Yamashita, A. Colombo, J.M. Tobis, Limitations of coronary angiography compared with intravascular ultrasound: implications for coronary interventions, Prog. Cardiovasc. Dis. 42 (2) (1999) 91–138.
[2] S.E. Nissen, P. Yock, Intravascular ultrasound: novel pathophysiological insights and current clinical applications, Circulation 103 (4) (2001) 604–616.

[3] N. Bom, W. Li, A.F. van der Steen, C.T. Lancee, E.I. Cespedes, C.J. Slager, C.L. de Korte, New developments in intravascular ultrasound imaging, Eur. J. Ultrasound 7 (1) (1998) 9–14.
[4] K. Rosenfield, D.W. Losordo, K. Ramaswamy, J.O. Pastore, R.E. Langevin, S. Razvi, B.D. Kosowsky, J.M. Isner, Three-dimensional reconstruction of human coronary and peripheral arteries from images recorded during two-dimensional intravascular ultrasound examination, Circulation 84 (5) (1991) 1938–1956.
[5] C. von Birgelen, R. Erbel, C. Di Mario, W. Li, F. Prati, J. Ge, N. Bruining, G. Gorge, C.J. Slager, P.W. Serruys, et al., Three-dimensional reconstruction of coronary arteries with intravascular ultrasound, Herz 20 (4) (1995) 277–289.
[6] F.A. Matar, G.S. Mintz, P. Douek, A. Farb, R. Virmani, S.P. Javier, J.J. Popma, A. D. Pichard, K.M. Kent, L.F. Satler, et al., Coronary artery lumen volume measurement using three-dimensional intravascular ultrasound: validation of a new technique, Cathet. Cardiovasc. Diagn. 33 (3) (1994) 214–220.
[7] E. Maurincomme, G. Finet, What are the advantages and limitations of the three-dimensional intracoronary ultrasound imaging?, in: J.H.C. Reiber, E. E. Van Der Wall (Eds.), Card. Imaging, Kluwer Academic, Publ., The Nederlands, 1996, pp. 243–255.
[8] J.L. Evans, K.H. Ng, S.G. Wiet, M.J. Vonesh, W.B. Burns, M.G. Radvany, B.J. Kane, C.J. Davidson, S.I. Roth, B.L. Kramer, S.N. Meyers, D.D. McPherson, Accurate three-dimensional reconstruction of intravascular ultrasound data. Spatially correct three-dimensional reconstructions, Circulation 93 (3) (1996) 567–576.
[9] M. Laban, J.A. Oomen, C.J. Slager, J.J. Wentzel, R. Krams, J.C.H. Schuurbiers, A. den Beer, C. von Birgelen, P.W. Serruys, P.J. de Feijter, ANGUS: a new approach to three-dimensional reconstruction of coronary vessels by combined use of angiography and intravascular ultrasound, in: Proceedings of the Computers in Cardiology, 1995, pp. 325–328.
[10] C.J. Slager, J.J. Wentzel, J.C. Schuurbiers, J.A. Oomen, J. Kloet, R. Krams, C. von Birgelen, W.J. van der Giessen, P.W. Serruys, P.J. de Feyter, True 3-dimensional reconstruction of coronary arteries in patients by fusion of angiography and IVUS (ANGUS) and its quantitative validation, Circulation 102 (5) (2000) 511–516.
[11] A.U. Coskun, Y. Yeghiazarians, S. Kinlay, M.E. Clark, O.J. Ilegbusi, A. Wahle, M. Sonka, J.J. Popma, R.E. Kuntz, C.L. Feldman, P.H. Stone, Reproducibility of coronary lumen, plaque, and vessel wall reconstruction and of endothelial shear stress measurements in vivo in humans, Cathet. Cardiovasc. Interv. 60 (1) (2003) 67–78.
[12] C.L. Feldman, A.U. Coskun, Y. Yeghiazarians, S. Kinlay, A. Wahle, M. E. Olszewski, J.D. Rossen, M. Sonka, J.J. Popma, J. Orav, R.E. Kuntz, P.H. Stone, Remodeling characteristics of minimally diseased coronary arteries are consistent along the length of the artery, Am. J. Cardiol. 97 (1) (2006) 13–16.
[13] S. Tu, N.R. Holm, G. Koning, Z. Huang, J.H. Reiber, Fusion of 3D QCA and IVUS/OCT, Int. J. Cardiovasc. Imaging 27 (2) (2011) 197–207.
[14] C.V. Bourantas, F.G. Kalatzis, M.I. Papafaklis, D.I. Fotiadis, A.C. Tweddel, I. C. Kourtis, C.S. Katsouras, L.K. Michalis, ANGIOCARE: an automated system for fast three-dimensional coronary reconstruction by integrating angiographic and intracoronary ultrasound data, Cathet. Cardiovasc. Interv. 72 (2) (2008) 166–175.
[15] G.D. Giannoglou, Y.S. Chatzizisis, G. Sianos, D. Tsikaderis, A. Matakos, V. Koutkias, P. Diamantopoulos, N. Maglaveras, G.E. Parcharidis, G. E. Louridas, In-vivo validation of spatially correct three-dimensional reconstruction of human coronary arteries by integrating intravascular ultrasound and biplane angiography, Coron. Artery Dis. 17 (6) (2006) 533–543.
[16] Y.S. Chatzizisis, G.D. Giannoglou, A. Matakos, C. Basdekidou, G. Sianos, A. Panagiotou, C. Dimakis, G.E. Parcharidis, G.E. Louridas, In-vivo accuracy of geometrically correct three-dimensional reconstruction of human coronary arteries: is it influenced by certain parameters? Coron. Artery Dis. 17 (6) (2006) 545–551.
[17] A. Wahle, P.M. Prause, S.C. DeJong, M. Sonka, Geometrically correct 3-D reconstruction of intravascular ultrasound images by fusion with biplane angiography–methods and validation, IEEE Trans. Med. Imaging 18 (8) (1999) 686–699.
[18] A. Wahle, M.E. Olszewski, M. Sonka, Interactive virtual endoscopy in coronary arteries based on multimodality fusion, IEEE Trans Med Imaging 23 (11) (2004) 1391–1403.
[19] ⟨http://www.paieon.com/Page.asp?Par=8.3&id=56⟩, (accessed 2013).
[20] Volcano Corporation and MediGuide Ltd. Announce Collaboration for Advanced Imaging and Navigation Technology, ⟨http://ir.volcanocorp.com/releasedetail.cfm?ReleaseID=215356⟩, (accessed 25.07.13.
[21] OpenCV, Open Source Computer Vision ⟨http://opencv.willowgarage.com/wiki/⟩, (accessed 25.07.13).
[22] Imebra, Open Source C++ Dicom library, http://imebra.com, accessed (accessed in 25.07.13).
[23] SISL, The SINTEF Spline Library, ⟨http://www.sintef.no/Projectweb/Geometry-Toolkits/SISL⟩, accessed (accessed 25.07.13).
[24] OpenGL, ⟨http://www.opengl.org⟩, accessed (accessed 25.07.13).
[25] C. de Boor, A Practical Guide to Splines, in, Springer Verlag, New York, 1978.
[26] M. Kass, A. Witkin, D. Terzopoulos, Snakes: active contour models, Int. J. Comput. Vision 1 (4) (1988) 321–331.
[27] G.D. Giannoglou, Y.S. Chatzizisis, V. Koutkias, I. Kompatsiaris, M. Papadogiorgaki, V. Mezaris, E. Parissi, P. Diamantopoulos, M.G. Strintzis, N. Maglaveras, G.E. Parcharidis, G.E. Louridas, A novel active contour model for fully automated segmentation of intravascular ultrasound images: in vivo validation in human coronary arteries, Comput. Biol. Med. 37 (9) (2007) 1292–1302.
[28] E. Parissi, Y. Kompatsiaris, Y. Chatzizisis, V. Koutkias, N. Maglaveras, M. Strintzis, G. Giannoglou, An automated model for rapid and reliable segmentation of intravascular ultrasound images, in: N. Maglaveras, I. Chouvarda, V. Koutkias, R.W. Brause (Eds.), Proceedings of the 7th International Symposium on Biological and Medical Data Analysis (ISB-MDA'06), Springer, Thessaloniki Greece, 2006, pp. 368–377.
[29] M. Papadogiorgaki, V. Mezaris, Y.S. Chatzizisis, G.D. Giannoglou, I. Kompatsiaris, Image analysis techniques for automated IVUS contour detection, Ultrasound Med. Biol. 34 (9) (2008) 1482–1498.
[30] R. Hartley, A. Zisserman, Multiple View Geometry in Computer Vision, 2nd ed., Cambridge University Press, 2004.
[31] J.S. Krouwer, Why Bland–Altman plots should use X, not (Y+X)/2 when X is a reference method, Stat. Med. 27 (5) (2008) 778–780.
[32] M. Sonka, R.W. Downe, J.W. Garvin, J. Lopez, T. Kovarnik, A. Wahle, IVUS-based assessment of 3D morphology and virtual histology: prediction of atherosclerotic plaque status and changes, in: Conference Proceedings—IEEE Engineering in Medicine and Biology Society, 2011, pp. 6647–6650.
[33] T.P. Exarchos, Y. Goletsis, K. Stefanou, E. Fotiou, D.I. Fotiadis, O. Parodi, Patient specific cardiovascular risk, assessment and treatment decision support based on multiscale modelling and medical guidelines, in: Conference Proceedings—IEEE Engineering in Medicine and Biology Society, 2011, pp. 838–841.
[34] G.D. Giannoglou, A.P. Antoniadis, Future trends in 3D intravascular ultrasound (IVUS) reconstruction, in: V.D. Tsakanikas, L.K. Michalis, D.I. Fotiadis, K. K. Naka, C.V. Bourantas (Eds.), Intravascular Imaging: Current Applications and Research Developments, IGI Global, Hershey, PA, 2012, pp. 355–359.
[35] J.D. Klingensmith, P. Schoenhagen, A. Tajaddini, S.S. Halliburton, E.M. Tuzcu, S. E. Nissen, D.G. Vince, Automated three-dimensional assessment of coronary artery anatomy with intravascular ultrasound scanning, Am. Heart J. 145 (5) (2003) 795–805.
[36] P.H. Stone, S. Saito, S. Takahashi, Y. Makita, S. Nakamura, T. Kawasaki, A. Takahashi, T. Katsuki, A. Namiki, A. Hirohata, T. Matsumura, S. Yamazaki, H. Yokoi, S. Tanaka, S. Otsuji, F. Yoshimachi, J. Honye, D. Harwood, M. Reitman, A.U. Coskun, M.I. Papafaklis, C.L. Feldman, Prediction of progression of coronary artery disease and clinical outcomes using vascular profiling of endothelial shear stress and arterial plaque characteristics: the prediCTION study, Circulation 126 (2) (2012) 172–181.
[37] R. Krams, J.J. Wentzel, J.A. Oomen, R. Vinke, J.C. Schuurbiers, P.J. de Feyter, P.W. Serruys, C.J. Slager, Evaluation of endothelial shear stress and 3D geometry as factors determining the development of atherosclerosis and remodeling in human coronary arteries in vivo. Combining 3D reconstruction from angiography and IVUS (ANGUS) with computational fluid dynamics, Arterioscler. Thromb. Vasc. Biol. 17 (10) (1997) 2061–2065.
[38] P. Siogkas, A. Sakellarios, T.P. Exarchos, L. Athanasiou, E. Karvounis, K. Stefanou, E. Fotiou, D.I. Fotiadis, K.K. Naka, L.K. Michalis, N. Filipovic, O. Parodi, Multiscale-patient-specific artery and atherogenesis models, IEEE Trans. Biomed. Eng. 58 (12) (2011) 3464–3468.
[39] Y.S. Chatzizisis, G.D. Giannoglou, Coronary hemodynamics and atherosclerotic wall stiffness: a vicious cycle, Med. Hypotheses 69 (2) (2007) 349–355.
[40] Y.S. Chatzizisis, A.U. Coskun, M. Jonas, E.R. Edelman, C.L. Feldman, P.H. Stone, Role of endothelial shear stress in the natural history of coronary atherosclerosis and vascular remodeling: molecular, cellular, and vascular behavior, J. Am. Coll. Cardiol. 49 (25) (2007) 2379–2393.
[41] A. Giannopoulos, Y.S. Chatzizisis, G.D. Giannoglou, Optical coherence tomography: an arrow in our quiver, Expert Rev. Cardiovasc. Ther. 10 (5) (2012) 539–541.